Design and Optimization of Hydraulic Buffer for a Sniper Grenade Launcher

Paihang Zhao, Yongjian Li, Dawei He, Junnuo Zhang, Penghan Gong

***Abstract*—Here, the optimal design of the hydraulic buffer is studied to reduce the recoil force of a sniper grenade launcher. According to the structural characteristics of the weapon, the installation scheme and size limitation of the hydraulic buffer are analyzed and calculated. The mathematical model of the hydraulic buffer is established, and the Runge-Kutta method is used. An optimization model is established based on design variables of the size and spacing of flow hole as well as objective values of buffer efficiency and effect. Moreover, the optimization model is obtained by a particle swarm optimization algorithm. The dynamic simulation and shooting test of the optimized scheme are conducted. The influence of hydraulic buffer on the movement of weapon components and its cushioning effect is compared with the original weapon. The results show that the hydraulic buffer can absorb some recoil energy of the automatic mechanism and reduce the peak velocity of each component. The peak recoil force and impulse of the weapon are reduced by 21.0% and 6.5%, respectively. The recoil impact of the weapon is effectively reduced by installing a hydraulic buffer.**

***Index Terms*—sniper grenade launcher; hydraulic buffer; PSO; optimization design; recoil force**

I. Introduction

In recent years, with the development of various recoil reduction technologies, various light weapons have been developed in the direction of high precision, large range, and low recoil. A sniper grenade launcher is a single-armed weapon for precise attack. Under the action of spring, rubber and other cushioning components, the recoil force can be greatly reduced, ensuring that it can be shot shoulder-to-shoulder. However, the recoil force is still larger than other shoulder-to-shoulder shooting weapons. It is necessary to find effective methods to further reduce the recoil force.

Hydraulic buffer is a device that converts mechanical energy into thermal energy using viscous damping of fluid flow. It can effectively reduce vibration and noise, decrease mechanical failure and prolong the service life of the equipment. Hydraulic buffer is intensively used in light weapons. Lin et al.[1] and Chen et al.[2] applied hydraulic buffer in a 12.7 mm rifle, which can significantly break the barrel recoil and reduce recoil forces. Gong et al.[[3] discussed the application of hydraulic buffer in an automatic grenade launcher, which can greatly reduce the recoil force. Zhang et al.[4] compared and analyzed the spring and hydraulic buffer on a hoe of a grenade launcher, and found that the effect of reducing recoil is the most obvious when using a hydraulic buffer. Duym and Raymond[5-7] studied the heat conduction law of the hydraulic buffer and proposed a new model based on heat conduction. Wang et al.[9] optimized the design of the multi-hole hydraulic buffer using an intelligent optimization algorithm, which improved the cushioning performance.

According to the structural characteristics of a sniper grenade launcher, the effective scheme of installed hydraulic buffer in the weapon by means of theoretical calculation, optimization design, simulation analysis and test verification is investigated in this study.

II. Structural Principle of a Sniper Grenade Launcher

A sniper grenade launcher belongs to a barrel short recoil, semi-free gun machine-type weapon, and its structural force sketch is shown in Fig.1. The main forces in the launcher are spring force, buffer force, bore force, resistance, support force of bracket and shoulder force of shooter.

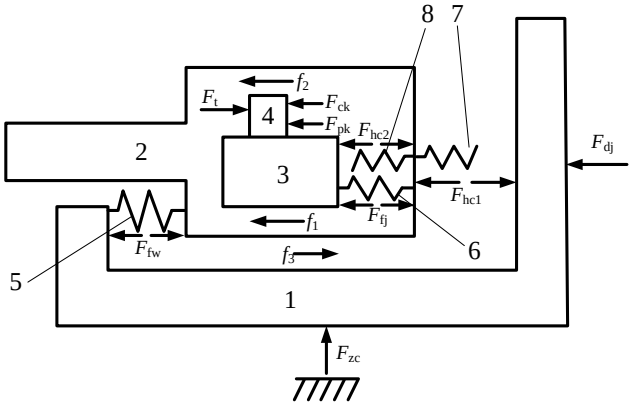

1-outer casing component; 2-barrel casing component; 3-automatic mechanism body; 4- automatic mechanism head; 5-return spring; 6-recoil spring; 7-cushion Ⅰ; 8-cushion Ⅱ

Fig.1 The force diagram of the launcher

Manuscript received June 14, 2019; revised December 23, 2019.

Paihang Zhao is with the Shijiazhuang Campus of Army Engineering University,Shijiazhuang,050003 and Information Engineering University,Zhengzhou,450001,China(e-mail:zhaopaihang@126.com).

Yongjian Li is with the Shijiazhuang Campus of Army Engineering University,Shijiazhuang,050003,China(Correspondent Author: phone:13231182695; e-mail:gunlyj@163.com).

Dawei He is with the Hu'nan Small Arms Research Institute CO.,LTD, Yiyang,413000, China. (e-mail:hk307470593@126.com).

Junnuo Zhang, is with the Shijiazhuang Campus of Army Engineering University,Shijiazhuang,050003,China(e-mail:junnuo556688@126.com).

Penghan Gong is with the Shijiazhuang Campus of Army Engineering University,Shijiazhuang,050003,China(e-mail:gongpenghan@126.com).

In Fig.1, F_{dj} is the shoulder force; F_{zc} is the support force of bracket; F_{hc1} is the cushion force between the casing and the outer casing; F_{hc2} is the cushion force between the automatic mechanism and casing; F_{fj} is the recoil spring force; F_{fw} is the return spring force; F_t is the bore force; F_{ck} is the pulling resistance; F_{pk} is the throwing resistance; f_1 is the friction force between the automatic mechanism body and casing; f_2 is the friction force between the automatic mechanism head and is casing; f_3 is the friction between the casing and the outer casing.

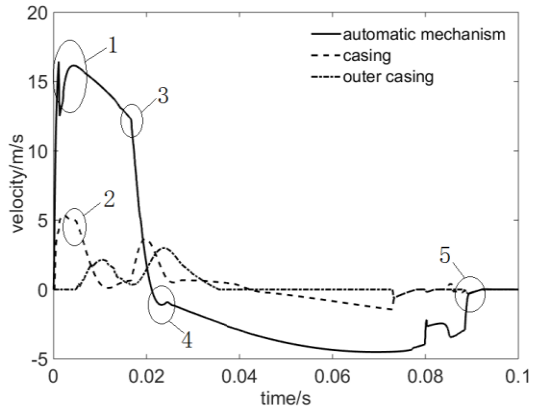

Fig.2 Velocity curves of components

The launcher is mainly composed of barrel and casing components, floating guide rail components, automation components, launcher components, cartridge drum, and bipod, etc. Because of the existence of many complex parts of the launcher and the model as well as the relatively weak modeling function of Adams software, Pro/E software is used to build its three-dimensional model, and Mechanism/Pro model is applied. Blocks are imported into Adams software to ensure the accuracy of the model.

In the process of modeling, the following simplifications and assumptions are made for weapon systems:

(1) Ignore the minor factors affecting the motion of the machine, merge components without relative motion, and ignore small mass non-critical parts;

(2) Without the consideration of the inertia of all springs, the spring damper is replaced by the spring damper in the software based on the type of springs.

(3) The launcher is a shoulder-to-shoulder launching weapon with small recoil force, and the ground support force has little influence on the shooting process when the shooting angle is zero. Therefore, the interaction between the hoe and soil is simplified to a common rigid body contact problem.

The velocity curves of the automatic mechanism, casing and outer casing of the launcher during the whole shooting cycle are shown in Fig.2. The muzzle direction of the launcher is set as the negative direction of motion. After the weapon is fired, the automatic mechanism drove the barrel casing to recoil together for a certain distance and then unlocked. The automatic mechanism continues to accelerate recoil under the bore force, until the mark 1, and the effect of the bore force ended. The casing recoils to the last place at mark 2, and then pushes the outer casing recoiling. The automatic mechanism reduces the recoil under the force of the recoil spring, friction, throwing and others. It recoils to the last place at the mark 3 and pushes the barrel casing recoiled, and the barrel casing pushes the outer casing recoiled. Under the recoil spring, the automatic mechanism starts to return at mark 4, and return to the place at mark 5, the shooting journey ends.

III. Buffer Design and Calculation

Hydraulic buffers use oil viscous to absorb mechanical energy into heat energy dissipation. The piston recovery process only has the spring elasticity, which provides less thrust back to its connecting parts. Therefore, it can be considered that hydraulic buffers could consume the most absorbed mechanical energy. In the shooting process of a weapon, the recoil kinetic energy of a weapon mainly comes from the impact between the casing and automatic machine. Therefore, a hydraulic buffer is added between them to absorb the recoil kinetic energy and reduce the recoil force.

A. Buffer Installation Scheme

Based on the gap in the middle of the sleeve, the hydraulic buffer is fixed at the bottom of the sleeve to alleviate the impact between the automatic machine and the casing. As shown in Fig.3(a), L1 is the automatic machine recoil stroke. When the automatic machine starts to recoil and the recoil stroke remains L2 (in Fig.3(b)), it contacts with the impact head of the hydraulic buffer, and starts to compress the piston rod of the hydraulic buffer. When the automatic machine finishes recoil, the buffer function of the hydraulic buffer is completed, as shown in Fig.3(c). Hence, the buffer stroke of the hydraulic buffer L3 should not less than L2. Therefore, the design scheme of the hydraulic buffer should satisfy the following conditions:

$$\begin{cases} L_3 \geq L_2 \\ \Phi_{hcq} < \varphi_{fjh} \end{cases} \quad (1)$$

Where Φ_{hcq} is the outer diameter of the hydraulic buffer, and φ_{fjh} is the inner diameter of the recoil spring.

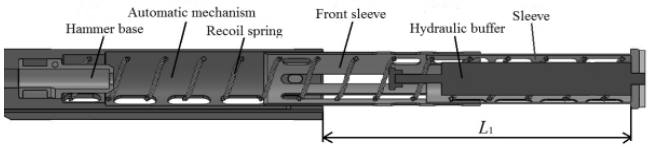

(a) The buffer mounting position

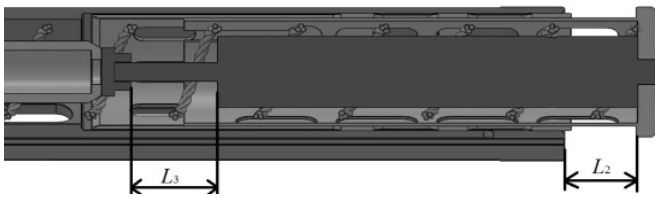

(b) The automatic machine recoiled to contact buffer

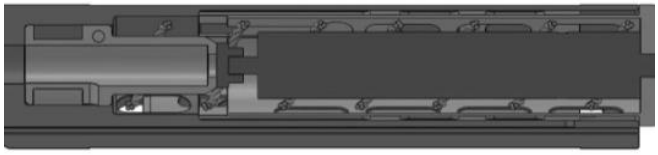

(c) The automatic machine recoiled to buffer function completed

Fig.3 The buffer stroke diagram of hydraulic buffer

B. The Structure Design of Hydraulic Buffer

Common hydraulic buffers include fixed orifice, multi-orifice, and throttle rod, etc. The fixed orifice is seldom used because of its uneven cushioning force. It is difficult to process a throttle rod type. Therefore, in this study, the porous hydraulic buffer is considered.

The structure principle of the multi-hole hydraulic buffer is shown in Fig.4. When the load is suddenly loaded on the piston rod, the hydraulic oil in the high-pressure chamber flows through the damping hole with high velocity. Because of the compressive and viscous action of the hydraulic oil, the mechanical energy of the impact load is transformed into the hydraulic energy, and the pressure energy is transformed into the thermal energy, which is eventually dissipated in the air.

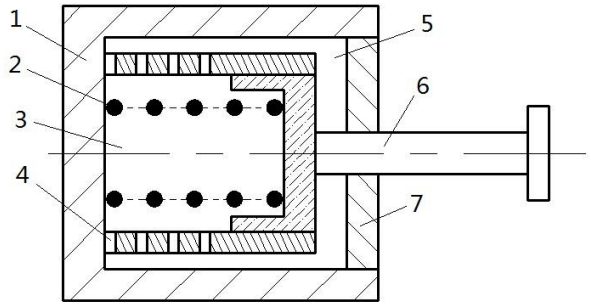

1. Cylinder block 2. Reset spring 3. High-pressure chamber 4. Damping hole 5. Low-pressure chamber 6. Piston rod 7. Cylinder head

Fig.4 The porous hydraulic buffer

C. Buffer design calculation

The mechanical analysis of the buffer is shown in Fig.5. Because the rear end of the buffer is connected with the sleeve and contacted with the rubber cushion, the hydraulic cushion is compressed at the same time when the automatic machine recoils in place. The mechanical model of the rubber cushion is simplified as a stiffness and damping system. The parameters of the system in the sense of minimum variance are obtained by fitting the test data as follows:

$$\begin{cases} m_t = 0.2(Kg) \\ C_1 = 55.71\left(\dfrac{N}{m/s}\right) \\ K_1 = 395.5(N/m) \end{cases} \quad (2)$$

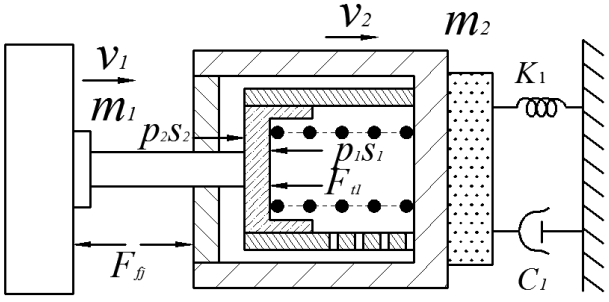

Fig.5 Force analysis of buffer

C1 Mathematical model

(1) Force Analysis of Piston Rod

After the automatic machine recoils in place and contacts the piston rod, the hydraulic buffer is compressed.

The motion equation of the piston rod is described as follows:

$$m_1 \frac{dv_1}{dt} = -p_1 s_1 - F_{t1} + p_2 s_2 - f_1 - f_2 - F_{fj} \quad (3)$$

Where m_1 is the mass of recoil body (automatic mechanism and piston rod); v_1 is the recoil velocity of the recoil; t is time; p_1 is the pressure of high-pressure chamber; s_1 is the cross-sectional area of high-pressure chamber; p_2 is the pressure of low-pressure chamber; s_2 is the effective area of piston in low-pressure chamber; f_1 and f_2 are friction forces between piston rod and cylinder head, plug and piston sleeve; F_{t1} is the spring force of the buffer reset spring; F_{fj} is the recoil spring force.

(2) Force Analysis of Buffer Cylinder

Rubber cushion is compressed by the cylinder block of the buffer, and the equation of motion is expressed as follows:

$$m_2 \frac{dv_2}{dt} = p_1 s_1 + F_{t1} - p_2 s_2 + f_1 + f_2 + F_{fj} - F_{xj1}$$
$$F_{xj1} = \begin{cases} 0 & , x_2 \le 0 \\ K_1 x_2 + C_1 v_2 & , x_2 > 0 \end{cases} \quad (4)$$

where m_2 is the mass sum of the cylinder body and sleeve of the buffer; F_{xj1} is the rubber cushion force; x_2 is the displacement of the cylinder body recoil; v_2 is the velocity of the cylinder body recoil.

(3) Flow Equation of Damping Hole

For thin-walled holes, the flow equation is expressed as follows:

$$q_1 = CA_c\sqrt{\frac{2(p_1 - p_2)}{\rho}} \quad (5)$$

where q_1 is the flow through the damper hole; C is the flow coefficient (0.60-0.62); A_c is the flow area through the damper hole; ρ is the density of hydraulic oil.

(4) Clearance Flow Equation of Piston and Piston Sleeve Fit

There is a fit clearance between the piston and piston tube, which leads to the formation of an annular gap. In addition, some oil would flow out of the gap. As shown in Fig.6, the flow equation of the gap is described as follows:

$$q_2 = \frac{\pi D \Delta p}{12\mu L}\delta^3 - \frac{\pi D v}{2}\delta \quad (6)$$

Where q_2 is the flow through the annular gap; D is the piston diameter; L is the piston width; δ is the piston and piston pipe clearance.

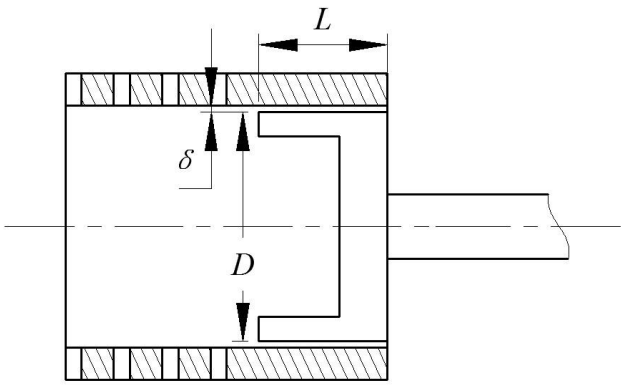

Fig.6 The diagram of piston and piston pipe fitting clearance

(5) Compressibility Equation of Hydraulic Oil

Because the oil pressure of the low-pressure chamber changes slightly during the buffer process, it is approximately considered that the oil pressure of the low-pressure chamber does not change. The volume of hydraulic oil varies with pressure. The compressibility equation is described as follows:

$$K = -V\frac{dp}{dV} \qquad (7)$$

where K is the bulk modulus of elasticity of oil and V is the volume of the high-pressure chamber.

After deduction, it can get:

$$\frac{dp}{dt} = -\frac{K}{V}\frac{dV}{dt} \qquad (8)$$

$$\frac{dV}{dt} = V_0 - (q_1 + q_2) \qquad (9)$$

Therefore, the differential equation of oil pressure in the high-pressure chamber can be obtained as follows:

$$\frac{dp_1}{dt} = -\frac{K(s_1 H - q_1 - q_2)}{s_1(H - x_1 + x_2)} \qquad (10)$$

where H is the length of the high-pressure chamber.

(6) Flow continuity equation

The continuity equation of oil flow in the piston tube is expressed as follows:

$$s_1(v_1 - v_2) = q_1 + q_2 \qquad (11)$$

(7) Flow-through Area Equation of Damping Hole:

$$A_c = A_c(x_1 - x_2) \qquad (12)$$

In summary, the differential equations of the buffer are expressed as follows:

$$\begin{cases} m_1\dfrac{dv_1}{dt} = -p_1 s_1 - F_{t1} + p_2 s_2 - f_1 - f_2 - F_{fj} \\ m_2\dfrac{dv_2}{dt} = p_1 s_1 + F_{t1} - p_2 s_2 + f_1 + f_2 + F_{fj} - F_{xj1} \\ \dfrac{dp_1}{dt} = -\dfrac{K(s_1 H - q_1 - q_2)}{s_1(H - x_1 + x_2)} \\ \dfrac{dx_1}{dt} = v_1 \\ \dfrac{dx_2}{dt} = v_2 \end{cases} \qquad (13)$$

C2 Simulation calculation

Input characteristic parameters contain C, ρ, μ, f_1, f_2, and K. Component parameters are m_1, m_2, p_{10}, p_{20}, and v_{20}. The flow hole area curve is expressed as $A_c(x_1\text{-}x_2)$. The initial velocity of piston rod motion is calculated by momentum conservation according to the recoil velocity of the automatic mechanism v_{10}. The fourth and fifth order Runge-Kutta methods with variable step size are used to solve the equations. As shown in Fig.7, the hydraulic resistance of the automatic mechanism recoil-in-place compression buffer can be obtained.

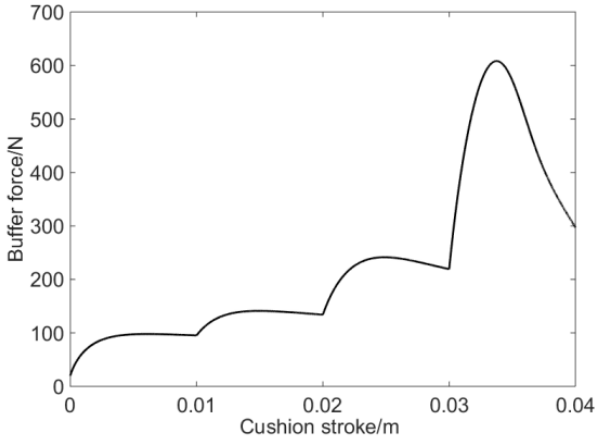

Fig.7 The hydraulic resistance curve

From Fig.7, it can be seen that the initial scheme of the buffer is remarkably different from the ideal damping curve of the buffer, and the buffer efficiency is not high. It is necessary to further optimize the buffer.

IV. Parameter Optimization

A. Optimizing Model

A1 Determination of Independent Variables

The buffer force curve of the porous hydraulic buffer is mainly related to the area and location of the flow hole. Therefore, the diameter and spacing of the flow hole are selected as optimization variables:

$$X = [d_1, d_i, \cdots, d_n, l_1, l_2, \cdots, l_n] \qquad (14)$$

where n is *the* number of holes; $d_i(i = 1, 2, \cdots, n)$ is the diameter of the i hole; $l_i(i = 1, 2, \cdots, n)$ is the distance between the first hole and the i hole; l_1 is the distance between the first hole and the end face of the piston at the initial position.

A2 Objective function

Buffer efficiency is used as an evaluation index for the buffer performance, and its calculation method is shown in formula (15). The buffer with high buffer efficiency could absorb more energy under the same buffer force and provide a better buffer effect.

$$\eta = \frac{\sum_{i=1}^{k} F(i)\cdot(x(i) - x(i-1))}{F_{\max}\cdot x_{\max}} \qquad (15)$$

where η is buffer efficiency; F is buffer force, and x is buffer stroke.

Due to the limited installation space of the buffer, the volume of the buffer is confined. However, the recoil velocity of the automatic mechanism is relatively high, and the hydraulic buffer could only absorb part of the energy of the automatic mechanism. While the residual kinetic energy is still absorbed by the buffer system of the weapon. Therefore, when the initial velocity is constant, the reduction of the velocity of the automatic mechanism after the buffer action is also regarded as an index to measure the performance of the buffer, which is called the buffer effect. In addition, its calculation method is shown in Equation (16). The bigger δ_v is, the more mechanical energy the buffer absorbed, the better the buffer effect.

$$\delta_v = \frac{v_0 - v_1}{v_0} \qquad (16)$$

Therefore, the linear proportional weighted summation method is used to set the objective function using the above two indicators. The calculation method is expressed as follows:

$$\max\ z = \omega_1 \eta + \omega_2 \delta_v \qquad (17)$$

where ω_1 and ω_2 are the weight of buffer efficiency and buffer effect, respectively. In order to focus on buffer effect, let $\omega_1 = 0.4$, $\omega_2 = 0.6$.

A3 Constraint condition

For the design of the hydraulic buffer scheme, a small aperture of throttle hole may lead to large cushioning force and difficult processing, and vice versa. Therefore, the following constraints should be considered comprehensively:

$$\begin{cases} 0.5 \le d_i (i = 1, 2, \cdots, n) \le 3 \\ 3 \le l_i (i = 1, 2, \cdots, n) \le 20 \\ \sum_{i=1}^{n} l_1 \le L - 3 \end{cases} \qquad (18)$$

where *L* is buffer travel length.

B. Optimizing Model

For the solution of the hydraulic bumper, it is necessary to use the cyclic iteration method of calling equations. The relationship between the objective function and independent variables is highly non-linear. Therefore, a stochastic algorithm without differentiability and continuity is adopted to solve this problem.

PSO is a group-based optimization tool with global optimization capability. Its algorithm flow is shown in Fig.8. Firstly, the algorithm initializes a group of stochastic solutions and reveals the optimal solution by iteration calculation. Then, it evaluates the individual fitness, compares with the initial objective function value, and preserves the particle with the smallest fitness. If it satisfies the stopping condition, the individual with the smallest output fitness will be saved. Otherwise, the position and velocity of the particle would be updated and iterated until the stopping criterion is satisfied.

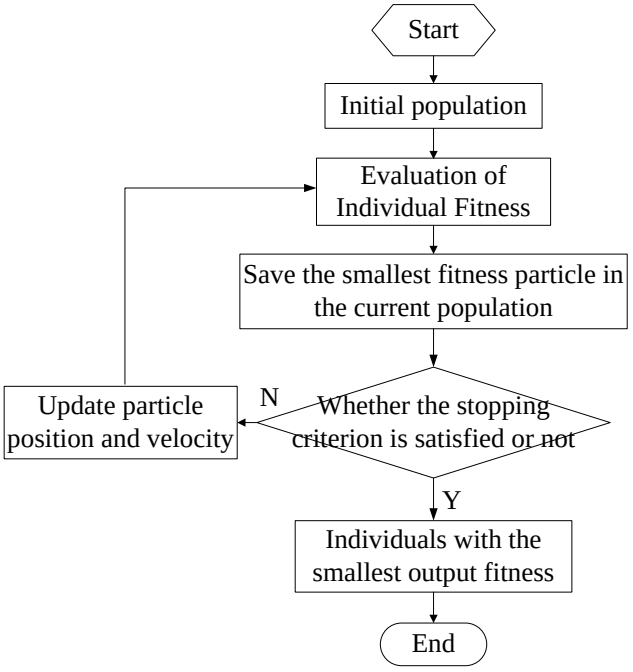

Fig.8 The flow chart of PSO

The mathematical description of PSO: In a D-dimensional space, a population of m particles is expressed as $X = (x_1, \cdots, x_i, \cdots, x_m)$, where the position of the *i* particle is $x_i = (x_{i1}, x_{i2}, \cdots, x_{iD})^{\mathrm{T}}$ and its velocity is $V_i = (v_{i1}, v_{i2}, \cdots, v_{iD})^{\mathrm{T}}$. Its individual extreme value is $p_i = (p_{i1}, p_{i2}, \cdots, p_{iD})^{\mathrm{T}}$; the global extreme value of the population is $p_g = (p_{g1}, p_{g2}, \cdots, p_{gD})^{\mathrm{T}}$. According to the principle of the following current optimal particle, the particle x_i would change its velocity and position based on formula (19) and formula (20).

$$v_{ij}(t+1) = \omega v_{ij}(t) + c_1 r_1 \left(p_{ij}(t) - x_{ij}(t) \right) + c_2 r_2 \left(p_{gj}(t) - x_{ij}(t) \right) \qquad (19)$$

$$x_{ij}(t+1) = x_{ij}(t) + v_{ij}(t+1) \qquad (20)$$

where $i = 1, 2, \cdots, m$, and $j = 1, 2, \cdots, D$. *m* is the population size; ω is inertial weight; t is current evolutionary algebra; r_1 and r_2 are random numbers between 0 and 1; c_1 and c_2 are the learning factors.

C. Optimized results

The number of iterations is 100, and the number of particles is 60 with PSO. The optimum number of fluid holes in buffer flow is 3, 4, 5 and 6. The optimum number of holes is 4. The optimum results are shown in Table 1. The optimized hydraulic resistance curve of the hydraulic buffer is displayed in Fig.9. Compared with Fig.7 and Fig.9, the hydraulic resistance of the hydraulic buffer is obviously smooth. Moreover, the buffer efficiency is increased from 0.435 to 0.882, and the buffer effect is improved from 0.142 to 0.261.

TABLE I
COMPARISON OF PARAMETERS BEFORE AND AFTER OPTIMIZATION

	Number of holes	aperture diameter	Hole position	Target variables
Before optimized	4	$\begin{cases} d_1=1 \\ d_2=1 \\ d_3=1 \\ d_4=1 \end{cases}$	$\begin{cases} l_1=10 \\ l_2=10 \\ l_3=10 \end{cases}$	0.259
After optimized	4	$\begin{cases} d_1=0.8 \\ d_2=0.8 \\ d_3=0.5 \\ d_4=2.6 \end{cases}$	$\begin{cases} l_1=3.1 \\ l_2=3.3 \\ l_3=7.9 \end{cases}$	0.509

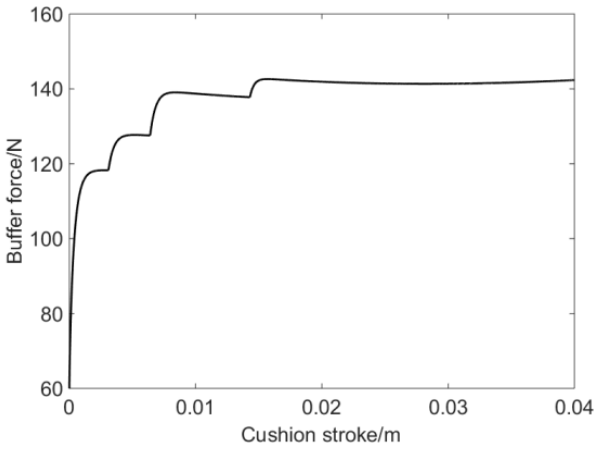

Fig.9 The hydraulic resistance curve after optimization

V. Parameter Optimization

A. Simulation analysis

The weight of the buffer is 300 g. In order to investigate the influence of the hydraulic buffer on the components of the weapon during launching, based on the virtual prototype model of the weapon[13], the buffer force of the hydraulic buffer is added to the model in the form of spline function between the automatic mechanism and casing. In addition, the mass block of 300 g is added to the casing to indicate the quality of the buffer. Then, the simulation analysis is conducted. Fig.10, 11 and 12 display motion contrast curves of automatic mechanism, casing and outer casing with or without hydraulic buffer, respectively.

Fig.10 shows that the velocity of the automatic mechanism has an obvious deceleration effect under the action of buffer force when the automatic mechanism recoils to the impact head of the hydraulic buffer. Fig.11 reveals that the peak velocity of the first recoil impact of the casing assembly decreases, and the velocity decreases correspondingly when the recoil energy remains unchanged due to the increased mass caused by the installation of the hydraulic buffer. Mark 2 is the second recoil of the barrel casing assembly driven by the automatic mechanism after the hydraulic buffer action. Because the hydraulic buffer absorbs partial automation energy, the energy acting on the casing decreases accordingly. Therefore, the recoil velocity of the casing also reduces to a certain extent. In Fig.12, the recoil kinetic energy of the casing component mark 1 decreases, resulting in a corresponding decrease in the recoil velocity of the outer casing. It suggests that the recoil velocity of the casing assembly and the outer casing assembly decreases correspondingly after the buffer action of the hydraulic buffer. The hydraulic buffer effectively absorbs some recoil energy and reduces the recoil impact between components.

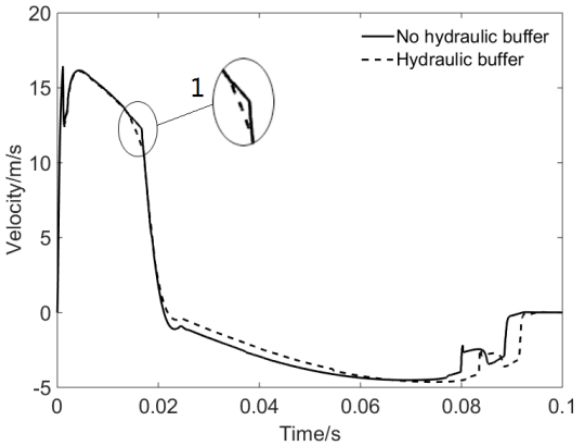

Fig.10 The contrast of motion curves of automatic mechanism

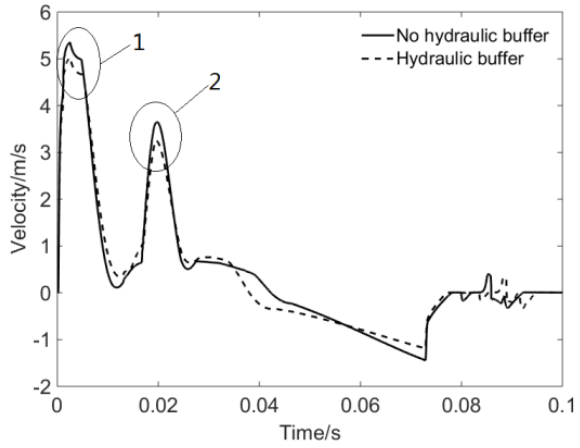

Fig.11 The contrast of motion curves of the casing

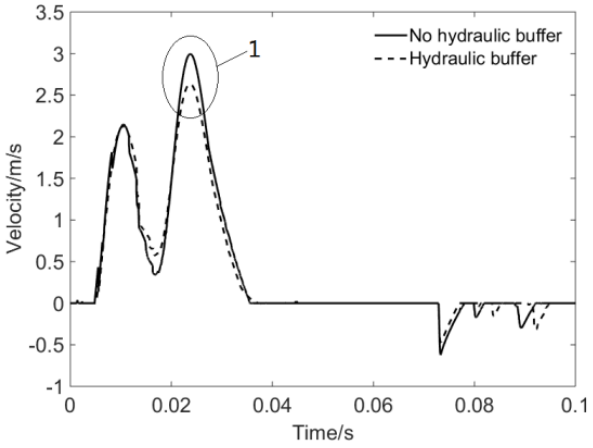

Fig.12 The contrast of motion curves of the outer casing

B. Shooting test

According to the optimized design scheme, the hydraulic cushion parts and assembly scheme are designed, which mainly consists of piston rod, cylinder head, oil storage cotton, piston, cylinder liner, cylinder block and reset spring. Its three-dimensional model is demonstrated in Fig.13, and its morphology is illustrated in Fig.14. The factory commissioned customized processing of hydraulic buffer parts, as shown in Fig.15.

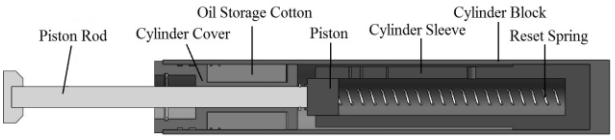

Fig.13 The structure composition of hydraulic buffer

Fig.14 The three-dimensional model of hydraulic buffer

Fig.15 The physical drawing of the hydraulic buffer

The launcher is fixed on the launcher. An AFT-L2 force sensor is installed between the tail end of the launcher and the shoulder bracket of the launcher. The data acquisition instrument record the sensor signals in the shooting process. The composition of the test system is revealed in Fig.16. The recoil force curve can be obtained by filtering and denoising the collected signals and unit conversion. Fig.17 and Fig.18 display the contrast of the recoil force curve and recoil impulse curve of primary launcher and launcher with the hydraulic buffer. The test results indicate that the peak recoil force of the weapon decreases by 21.0% and the recoil impulse of a firing cycle decreases by 6.5%.

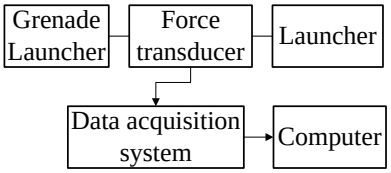

Fig.16 The recoil force testing system

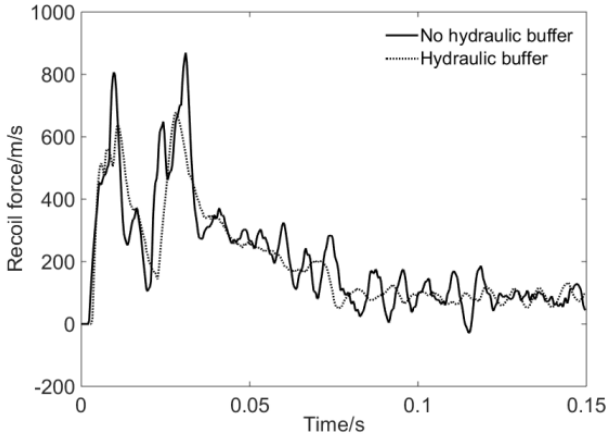

Fig.17 The recoil force contrast curve

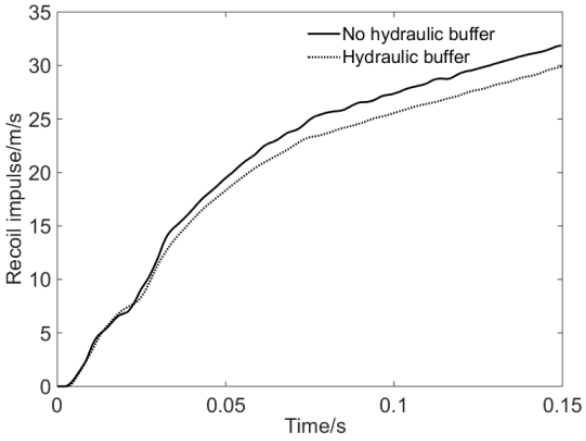

Fig.18 The recoil impulse contrast curve

VI. Conclusion

According to the structural characteristics of a sniper grenade launcher, a hydraulic buffer is designed, which is installed between the automatic mechanism and the casing and used for buffer the recoil velocity of automatic mechanism. The mathematical model of the hydraulic cushion is established using the related theories of dynamics, newton mechanics and hydrodynamics. The optimal design scheme is obtained by taking the diameter and spacing of the fluid hole as independent variables and the cushion efficiency and cushion effect as objective variables.

The dynamic simulation analysis of the optimized buffer scheme reveals that the hydraulic buffer could absorb a part of the recoil energy of the automatic mechanism, reducing the recoil velocity of the casing and the outer casing, and the impact between the components is decreased. The results show that the peak recoil force could be reduced by 21.0%, and the recoil impulse could be reduced by 6.5%. The recoil impact of the weapon could be effectively reduced, and the comfort of the shooter could be improved.

REFERENCES

[1] L REN, G WANG, “Buffer design and Simulation of large caliber rifle based on AMESI,” Journal of Ordnance Equipment Engineering, 2016, (3),pp45-48.

[2] X L CHEN, “Buffer design and dynamics simulation of Chen Xianlei's 12.7mm sniper rifle,” Taiyuan: Zhongbei University, 2017.

[3] P H GONG, Y J LI, J X CHEN, “Buffer design and dynamics simulation of an automatic grenade launcher,” Chinese Hydraulics & Pneumatics, 2011, (3),pp7-9.

[4] T ZHANG, Z Q LIAO, J TANG. “Research on the Buffer Launch Technology for a Grenade Launcher,” Machine Design and Manufacturing Engineering, 2014, (1),pp24-27.

[5] DUYM S,STIENS R,REYBRIUCK K, “Evaluation of Shock Absorber Models”, Vehicle System Dynamics,1997,27(02), pp109 －127.

[6] DUYM S, “Simulation Tools Modeling and Identification for an Automotive Shock in the Context of Vehicle Dynamics,” Vehicle System Dynamics,2000,33(4),pp261－285.

[7] RAYMOND MARTHA K, “Shock Absorber Takes the Heat,” Machine Design,1977,69(4),pp64－64.

[8] Christof Rohrig, and Daniel HeB, "OmniMan: An Omnidirectional Mobile Manipulator for Human-Robot Collaboration," Lecture Notes in Engineering and Computer Science: Proceedings of The International MultiConference of Engineers and Computer Scientists 2019, 13-15 March, 2019, Hong Kong, pp55-60.

[9] C L WANG,Z W QIU, Q L ZENG, “Damping hole optimization of porous hydraulic buffer based on simulated annealing algorithm,” Chinese Hydraulics & Pneumatics, 2019, (4),pp 54-59.

[10] X YANG, X W ZHANG, X F WANG, “The Optimizing Design Oil Shock Absorber,” Chinese Hydraulics & Pneumatics,2003,26(4), pp33-35.

[11] S SUN, “Simulation and Optimum Design to the Multi－orifice Hydraulic Buffer,” Dalian: Dalian University of Technology,2006.

[12] KASTEEL V R, “A New Shock Absorber Model for Use in Vehicle Dynamic Studies,” Vehicle System,2005,30(13), pp13-20.

[13] W Y WU, “Fluid Dynamics,” Beijing: Peking University Press, 2006.

[14] Christof Rohrig, and Daniel HeB, "OmniMan: An Omnidirectional Mobile Manipulator for Human-Robot Collaboration," Lecture Notes in Engineering and Computer Science: Proceedings of The International MultiConference of Engineers and Computer Scientists 2019, 13-15 March, 2019, Hong Kong, pp55-60

[15] P H ZHAO, R L WANG, Y J LI, “Study on the influence of rubber buffer parts on the launching performance of a sniper grenade launcher,” Journal of vibration and shock, 2018, (23), pp241-246.

[16] Seobi T , Anderson S H , Udawatta R P , “Influence of Grass and Agroforestry Buffer Strips on Soil Hydraulic Properties for an Albaqualf,” Soil Science Society of America Journal, 2005, 69(3),pp893.

[17] S FENG, “60 mm Automatic Light Motor Recoil Buffer and Traversing Mechanism Design and Research,” Shenyang: Dongbei University,2013.

[18] R T LI, G F CHEN, P LIANG, “Modeling and Finite Element Analysis of the Hydraulic Buffer in Elevator Systems,” Journal of Civil Engineering Research 2017, 7(2),pp63-66.

[19] Wenjun Y , Yinwei Y , Zhanyu W, “Parameters Optimization of a Hydraulic Buffer System for Belt Arrestor in Downward Belt Conveyors,” Mathematical and Computational Applications, 2016, 21(4),pp42-54.

[20] Y L LI , Z Q LIU, “Research and Design on Multi-orifice Hydraulic Buffer,” Hydraulics Pneumatics & Seals, 2014.

[21] Yi-Cheng Lee, and Syh-Shiuh Yeh, "Using Machine Vision to Develop an On-Machine Thread Measurement System for Computer Numerical Control Lathe Machines," Lecture Notes in Engineering and Computer Science: Proceedings of The International MultiConference of Engineers and Computer Scientists 2019, 13-15 March, 2019, Hong Kong, pp67-72

[22] K. Kankhunthodl, V. Kongratana, A. Numsomran, and V. Tipsuwanporn, "Self-balancing Robot Control Using Fractional-Order PID Controller," Lecture Notes in Engineering and Computer Science: Proceedings of The International MultiConference of Engineers and Computer Scientists 2019, 13-15 March, 2019, Hong Kong, pp77-82